TCTEX1D4, a novel protein phosphatase 1 interactor: connecting the phosphatase to the microtubule network

Luís Korrodi-Gregório[1], Sandra I. Vieira[2], Sara L. C. Esteves[1], Joana V. Silva[1], Maria João Freitas[1], Ann-Kristin Brauns[3], Georg Luers[3], Joana Abrantes[4,5], Pedro J. Esteves[4,6], Odete A. B. da Cruz e Silva[2], Margarida Fardilha[7,*] and Edgar F. da Cruz e Silva[1,‡]

[1]Laboratory of Signal Transduction, Centre for Cell Biology, Biology Department, University of Aveiro, 3810-193 Aveiro, Portugal
[2]Laboratory of Neurosciences, Centre for Cell Biology, Health Sciences Department and Biology Department, University of Aveiro, 3810-193 Aveiro, Portugal
[3]Department of Anatomy and Experimental Morphology, Center of Experimental Medicine, University Medical Center Hamburg-Eppendorf, D-20246 Hamburg, Germany
[4]CIBIO-UP, Centro de Investigação em Biodiversidade e Recursos Genéticos – Universidade do Porto, Campus Agrário de Vairão, Rua Padre Armando Quintas, número 7, 4485-661 Vairão, Portugal
[5]INSERM, U892, Université de Nantes, 44007 Nantes, France
[6]CITS, Centro de Investigação em Tecnologias de Saúde, CESPU, 4585-116 Gandra, Portugal
[7]Laboratory of Signal Transduction, Centre for Cell Biology, Biology Department and Health Sciences Department, University of Aveiro, 3810-193 Aveiro, Portugal

*Author for correspondence (mfardilha@ua.pt)
‡Deceased 2nd March 2010

Summary

Reversible phosphorylation plays an important role as a mechanism of intracellular control in eukaryotes. PPP1, a major eukaryotic Ser/Thr-protein phosphatase, acquires its specificity by interacting with different protein regulators, also known as PPP1 interacting proteins (PIPs). In the present work we characterized a physiologically relevant PIP in testis. Using a yeast two-hybrid screen with a human testis cDNA library, we identified a novel PIP of PPP1CC2 isoform, the T-complex testis expressed protein 1 domain containing 4 (TCTEX1D4) that has recently been described as a Tctex1 dynein light chain family member. The overlay assays confirm that TCTEX1D4 interacts with the different spliced isoforms of PPP1CC. Also, the binding domain occurs in the N-terminus, where a consensus PPP1 binding motif (PPP1BM) RVSF is present. The distribution of TCTEX1D4 in testis suggests its involvement in distinct functions, such as TGFβ signaling at the blood–testis barrier and acrosome cap formation. Immunofluorescence in human ejaculated sperm shows that TCTEX1D4 is present in the flagellum and in the acrosome region of the head. Moreover, TCTEX1D4 and PPP1 co-localize in the microtubule organizing center (MTOC) and microtubules in cell cultures. Importantly, the TCTEX1D4 PPP1BM seems to be relevant for complex formation, for PPP1 retention in the MTOC and movement along microtubules.

These novel results open new avenues to possible roles of this dynein, together with PPP1. In essence TCTEX1D4/PPP1C complex appears to be involved in microtubule dynamics, sperm motility, acrosome reaction and in the regulation of the blood–testis barrier.

Introduction

Reversible protein phosphorylation is a post-transcriptional event that is regulated by both protein kinases and phosphatases (PPs). This is a crucial intracellular control mechanism in eukaryotes, being involved in almost all cellular functions, from metabolism to signal transduction and cell division (Cohen, 2002). Phosphoprotein phosphatase 1 (PPP1), one of the major eukaryotic Ser/Thr-PPs, has exquisite specificities in vivo, both in terms of substrates and cellular localization. Over the past two decades, it has become apparent that PPP1 versatility is achieved by its ability to interact with multiple targeting/regulatory subunits known as PPP1 interacting proteins – PIPs (Cohen, 2002; Virshup and Shenolikar, 2009). PPP1 catalytic subunit (PPP1C) is encoded by three different genes giving rise to α/A, β/B, and γ/C isoforms. After transcription, PPP1CC undergoes tissue-specific splicing, originating a ubiquitously expressed isoform, PPP1CC1 and a testis-enriched and sperm-specific isoform, PPP1CC2 (da Cruz e Silva et al., 1995).

To date, more than 200 PIPs have been identified, most of them having the consensus PPP1 binding motif (PPP1BM) RVxF that binds to the catalytic subunit of PPP1, determining its function and specific cellular location (Fardilha et al., 2010; Hendrickx et al., 2009). Several PPP1-PIP complexes are involved in cytoskeleton functions. For instance, PPP1-Phostensin holoenzyme has been

implicated in actin rearrangements (Kao et al., 2007). Phostensin targets PPP1 to F-actin, being an actin filament pointed end-capping protein that is capable of modulating actin dynamics (Lai et al., 2009). The protein family PHACTR (all members 1–4) is involved in synaptic activity through the control of the actin cytoskeleton and by regulating PPP1 and actin (Allen et al., 2004). The above mentioned PIPs bind actin through the amino acids Arg–Pro–Glu–Leu and may direct PPP1 to a panoply of actin-associated substrates. Thus, several lines of evidence imply PPP1 in the regulation of cytoskeleton dynamics, together with various PIPs. This not only occurs at the actin level but also at the tubulin level. PPP1 has been shown to be anchored to *Chlamydomonas* central pair apparatus axoneme, associated with the C1 microtubule, and to a lesser extent to the outer doublet microtubules, suggesting that PPP1 can control both dynein arms and thereby flagellar motility (Yang et al., 2000). Also, recent data from our laboratory showed that PPP1 co-immunoprecipitates with tubulin from human sperm (Fardilha et al., 2011b).

Clearly the key to characterize the diverse roles of PPP1 relies on the identification of novel PIPs, and in the understanding of the specific functions of these complexes. Therefore, we focused on the identification of novel PIPs, through yeast two-hybrid screens where PPP1CC isoforms were used as baits (Browne et al., 2007; Fardilha et al., 2011b; Fardilha et al., 2004; Wu et al., 2007). In this study, we present a novel partner of PPP1, the T-complex testis expressed protein 1 domain containing 4 (TCTEX1D4/Tctex2β), which has recently been described as a novel Tctex1 dynein light chain family member (Meng et al., 2006). Further, the TCTEX1D4/PPP1CC subcellular co-localization and its dependence on TCTEX1D4-PPP1CC binding, support functions for the complex in microtubules dynamics. Simultaneously, the data also contribute to our understanding of the molecular basis of sperm motility as well as the dynamic and varied functional nature of PPP1.

Results

Identification and *in silico* characterization of TCTEX1D4, a novel PPP1CC binding protein

A yeast two-hybrid screen was performed against a human testis cDNA library using the C-terminus portion of PPP1CC2 as bait (Fardilha et al., 2011b). Four clones were obtained encoding the T-complex testis expressed protein 1 domain 4 (TCTEX1D4). TCTEX1D4 is a novel member of the dynein LC Tctex1 family that was recently identified as a binding partner of endoglin, a transmembranar glycoprotein involved in the transforming growth factor β (TGFβ) signaling (Meng et al., 2006). TCTEX1D4 has 221 amino acids, with an expected molecular mass of 23352 Da. The gene maps to human chromosome 1p34.1 and has 2 exons (Meng et al., 2006).

In order to identify physiologically relevant motifs and phosphorylation sites from the signaling perspective, we performed a bioinformatic analysis using the human TCTEX1D4 protein sequence in ELM (Puntervoll et al., 2003), PsiPred (Jones, 1999), ScanProsite, NetPhos and NetNGlyc1.0 servers. The conservation of motifs identified was analyzed by comparison with other mammalian sequences, and only results with high scores are shown. Based in ELM and Psipred, the TCTEX1D4 sequence was first divided into two domains: the disordered domain (residues 1 to 95) and the globular domain (residues 96 to 221) (Fig. 1A). Secondary structure prediction of the globular domain suggests two alpha helices, followed by four

β strands resembling that of DYNLT1. Since amino acids from the disordered domain should be more accessible to kinases and phosphatases, only the putatively phosphorylatable motifs of the disordered domain are shown in Fig. 1A. The bioinformatic approach revealed that the TCTEX1D4 disordered domain contains many putative Ser phosphorylation sites, such as consensus sites for protein kinase A (PKA, Ser24/53/66/92), B (PKB, Ser53/66) and C (PKC, Ser49), cyclin dependent kinase 1 (CDK1, Ser24), casein kinase 1 (CK1, Ser92) and 2 (CK2, Ser34), mitogen-activated protein kinase (MAPK, Ser24), and glycogen synthase kinase 3 (GSK3, Ser49). Remarkably, no potential Thr and Tyr phosphorylation sites were found.

The NetNGlyc1.0 server indicated a putative N-glycosylation motif in the extreme C-terminus (residues 205 to 210). Putative binding domains were also identified for the motif "anaphase-promoting complex (APC/C) binding site through the destruction box" (residues 28 to 36), for cyclins (residues 161 to 165), for MAPK (residues 167 to 176) (Fig. 1A). Additionally and particularly relevant to PIPs, the canonical PPP1BM RVxF was detected in the bioinformatics analysis, [90]RVSF[93], and reinforces the assertion that TCTEX1D4 is a PPP1 binding partner (Fig. 1A).

TCTEX1D4 belongs to the Tctex1 family of dynein LCs that share the Tctex1 globular domain, a region of high homology present among the different family members (Fig. 1). The human Tctex1 family comprises 6 members: DYNLT1 (Tctex1), DYNLT3 (RP3), TCTEX1D1, TCTEX1D2 (Tctex2b), TCTEX1D3 (Tctex2/Tcte3), and TCTEX1D4 (Tctex2β). A ClustalW2 protein alignment with full-length protein sequences (Fig. 1B) revealed that the Tctex1 domain is common to all proteins studied. A score of 57% was obtained between DYNLT1 and DYNLT3 when using only the TCTEX1 globular domain. For the other four family members of the Tctex1 domain containing proteins, the score varied between 25% and 33% (alignment not shown). This implies the formation of two distinct groups, one that contains DYNLT1 and DYNLT3 and one that contains the Tctex1 domain containing proteins. These results are in accordance with the work of DiBella and Meng (DiBella et al., 2004; Meng et al., 2006).

Since reversible protein phosphorylation is an important mechanism involved in the control of dynein function (Vaughan et al., 2001; Wirschell et al., 2007), a bioinformatics analysis was carried out for all the PPP1 binding motifs known in all dynein LCs, light intermediate chains (LICs), and intermediate chains (ICs) (Pazour et al., 2006). Interestingly, from all LCs, besides TCTEX1D4, only TCTEX1D3 possesses a consensus PPP1BM (Fig. 1B,C). Between the ICs and LICs, the IC2, DYNC1LI1 and DYNC1LI2 proteins also have a canonical PPP1BM.

In order to evaluate the evolutionary conservation of the phosphorylation sites and motifs described above (Fig. 1A), a ClustalW2 alignment was performed using representative orthologs of TCTEX1D4 (Fig. 2A). A phylogenetic tree was further constructed using either the Neighbor-Joining or the Maximum likelihood methods (given the similar results, only one of the methods is shown), revealing that TCTEX1D4 follows the modern mammalian taxonomy (Fig. 2B). Besides being present in placental mammals, TCTEX1D4 is also present in marsupials (*Monodelphis domestica*) and monotremes (*Ornithorhynchus anatinus*), birds (*Gallus gallus*) and fishes (*Danio rerio*, outgroup of the evolutionary tree). The results
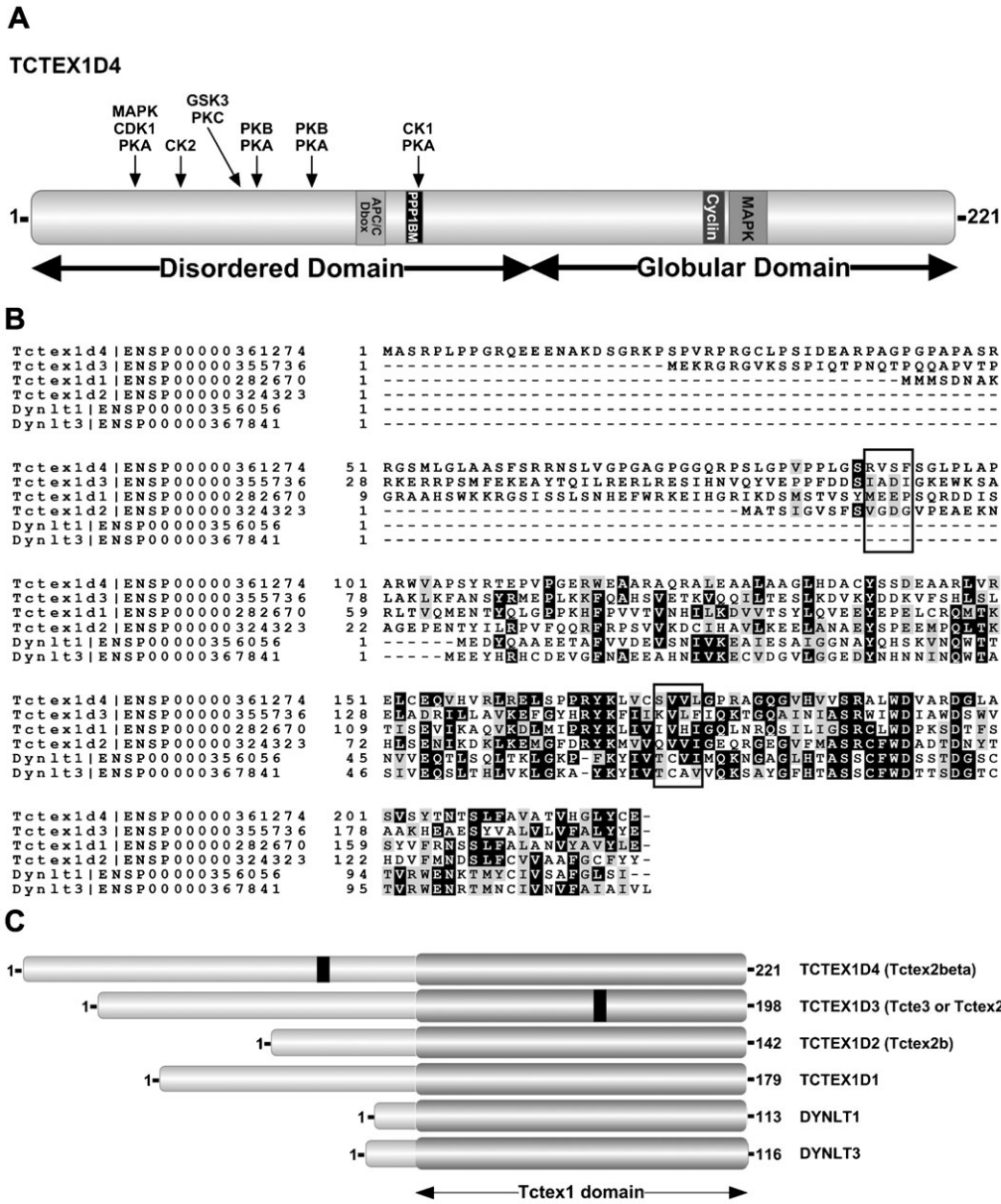
A

TCTEX1D4

B

```
Tctex1d4|ENSP00000361274    1  MASRPLPPGRQEEENAKDSGRKPSPVRPRGCLPSIDEARPAGPGPAPASR
Tctex1d3|ENSP00000355736    1  ----------------------MEKRGRGVKSSPIQTPNQTPQQAPVTP
Tctex1d1|ENSP00000282670    1  -----------------------------------------MMMSDNAK
Tctex1d2|ENSP00000324323    1  -------------------------------------------------
Dynlt1|ENSP00000356056      1  -------------------------------------------------
Dynlt3|ENSP00000367841      1  -------------------------------------------------

Tctex1d4|ENSP00000361274   51  RGSMLGLAASFSRRNSLVGPGAGPGGQRPSLGPVPPLGSRVSFSGLPLAP
Tctex1d3|ENSP00000355736   28  RKERRPSMFEKEAYTQILRERLRESIHNVQYVEPFDDSIADIGKEWKSA
Tctex1d1|ENSP00000282670    9  GRAAHSWKKRGSISSLSNHEFWRKEIHGRIKDSMSTVSYMEEPSQRDDIS
Tctex1d2|ENSP00000324323    1  -----------------MATSIGVSFSVGDGVPEAEKN
Dynlt1|ENSP00000356056      1  -------------------------------------------------
Dynlt3|ENSP00000367841      1  -------------------------------------------------

Tctex1d4|ENSP00000361274  101  ARWVAPSYRTEPVPGERWEAARAQRALEAALAAGLHDACYSSDEAARLVR
Tctex1d3|ENSP00000355736   78  LAKLKFANSYRMEPLKKFQAHSVETKVQQILTESLKDKVFSHLSL
Tctex1d1|ENSP00000282670   59  RLTVQMENTYQLGPPKHFPVVTVNHILKDVVTSYLQVEEYEPELCRQMTK
Tctex1d2|ENSP00000324323   22  AGEPENTYILRPVFQQRFRPSVVKDCIHAVLKEELANAEYSPEEMPQLTK
Dynlt1|ENSP00000356056      1  ------MEDYQAAEETAFVVDEVSNIVKEAIESAIGGNAYQHSKVNQWTT
Dynlt3|ENSP00000367841      1  -----MEEYHRHCDEVGFNAEEAHNILVKECVDGVLGGEDYNHNNINQWTA

Tctex1d4|ENSP00000361274  151  ELCEQVHVRLRELSPPRYKLVCSVVLGPRAGQGVHVVSRALWDVARDGLA
Tctex1d3|ENSP00000355736  128  ELADRILLAVKEFGYHRYKFIIKVLFIQKTGQAINIASRWIWDIAWDSWV
Tctex1d1|ENSP00000282670  109  TISEVIKAQVKDLMIPRYKLIVIVHIGQLNRQSILIGSRCLWDPKSDTFS
Tctex1d2|ENSP00000324323   72  HLSENIKDKLKEMGFDRYKMVVQVVIGEQRGEGVFMASRCFWDADTDNYT
Dynlt1|ENSP00000356056     45  NVVEQTLSQLTKLGKP-FKYIVTCVIMQKNGAGLHTASSCFWDSSTDGSC
Dynlt3|ENSP00000367841     46  SIVEQSLTHLVKLGKA-YKYIVTCAVVQKSAYGFHTASSCFWDTTSDGTC

Tctex1d4|ENSP00000361274  201  SVSYTNTSLFAVATVHGLYCE-
Tctex1d3|ENSP00000355736  178  AAKHEAESYVALVLVFALYYE-
Tctex1d1|ENSP00000282670  159  SYVFRNSSLFALANVYAVYLE-
Tctex1d2|ENSP00000324323  122  HDVFMNDSLFCVVAAFGCFYY-
Dynlt1|ENSP00000356056     94  TVRWENKTMYCIVSAFGLSI--
Dynlt3|ENSP00000367841     95  TVRWENRTMNCIVNVFAIAIVL
```

C

Fig. 1. **Schematic representation of the human TCTEX1D4 and its family members.** The human sequences of Tctex1 family proteins were obtained from Ensembl database. (**A**) The human protein sequence of TCTEX1D4 was submitted to ELM to appoint relevant motifs. TCTEX1D4 disordered (amino acids 1–95) and globular domains (amino acids 96–221) are shown. Putative conserved motifs and phosphorylation sites for specific kinases are indicated. (**B**) Sequences were submitted to ClustalW2 and the resulting aligning output file shaded with BOXSHADE. Open squares indicate the PPP1BM RVSF of TCTEX1D4 and the KVLF motif of TCTEX1D3. (**C**) Schematic representation of human Tctex1 family members with their respective TCTEX1 globular domains (dark gray). The black squares show the position of the PPP1BM of TCTEX1D4 and TCTEX1D3.

show that phosphorylation sites Ser34/49/53/66, consensus sites for CK2, GSK3, PKA, PKB and PKC, are conserved in all mammals, Ser92 is present in all mammals except for pig (*Sus scrofa*) and kangaroo rat (*Dipodomys ordii*), and Ser24 is present in all primates (except *Microcebus murinus*, a representative of lower primates Stepsirrhini, lemurs), Artiodactyla, Carnivora (except dog, *Canis familiaris*) and Chiroptera. The N-glycosylation motif is highly conserved in mammals but not in Murinae. The APC/C binding site is conserved in all mammals with the exception of *Cavia porcellus*. The cyclins binding site is present in all mammals but not in *Felis catus*, Insectivora and Rodentia (excluding *Dipodomys ordii*), and the MAPK binding site is conserved in all mammals, fish and birds. Finally, the PPP1BM is conserved in all placental mammals, with the exception of *Pteropus vampyrus* from the order Chiroptera (Fig. 2A).

Validation of the TCTEX1D4–PPP1 interaction

To prove the interaction between TCTEX1D4 and PPP1C isoforms, AH109 yeast strain was co-transformed with pACT-2-TCTEX1D4 and with *PPP1CA*, *PPP1CC1*, *PPP1CC2* or the *PPP1CC2end* in pAS2-1 (Fardilha et al., 2004; Fardilha et al., 2011b). After growing in selective media, colonies were transferred to plates with X-α-Gal, and all colonies turned blue, indicating that TCTEX1D4 interacts with the PPP1C isoforms (Fig. 3A).

The existence of TCTEX1D4-PPP1 complexes *in vivo* was shown by co-immunoprecipitation of the latter from cell lysates of COS-7 that were transfected with Myc-TCTEX1D4 (Fig. 3B). When PPP1CC was immunoprecipitated from cells transfected with Myc-TCTEX1D4, the protein was highly co-immunoprecipitated, as denoted by the intense Myc-immunopositive band in Western blot analysis (Fig. 3B).
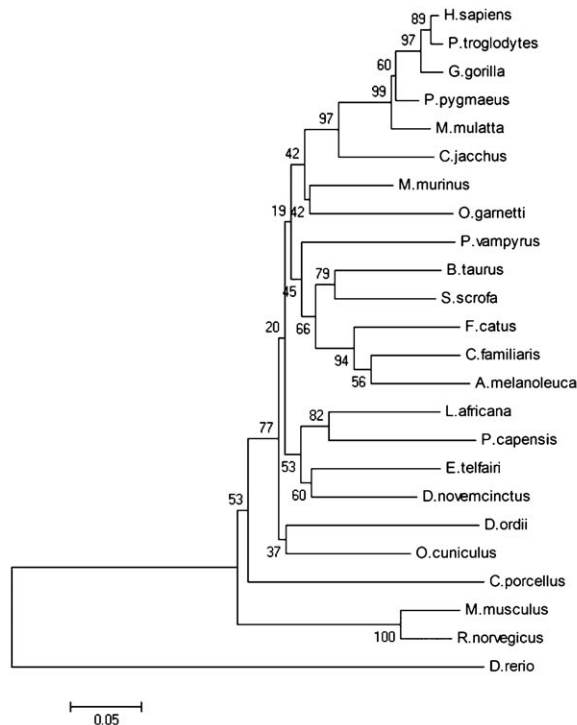
Biology Open

A
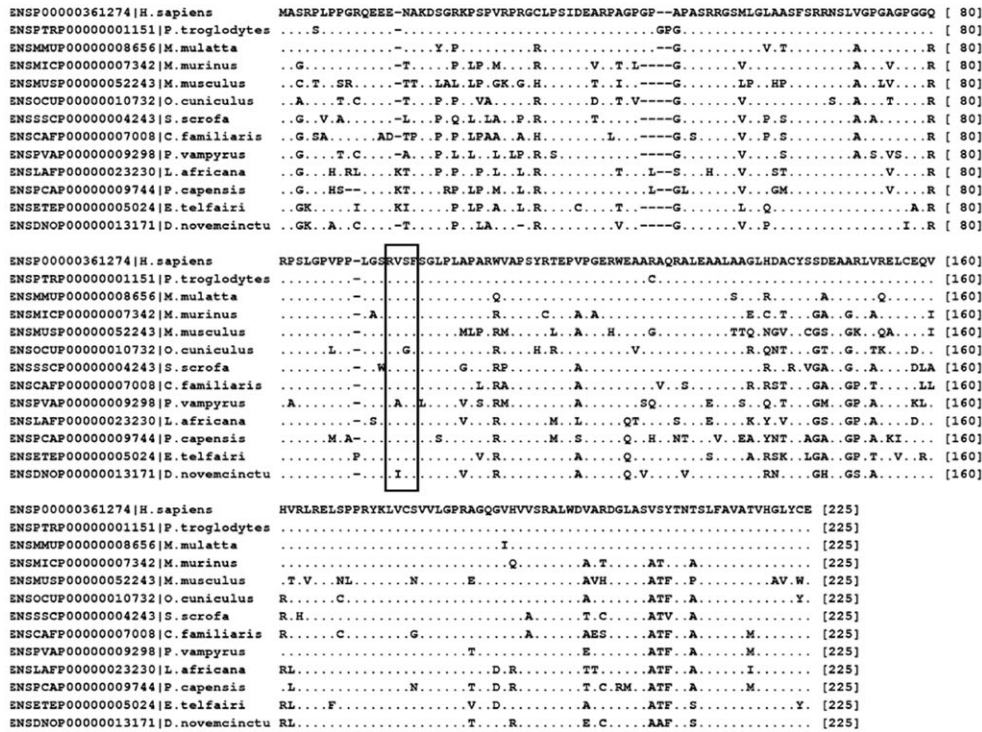
B

Fig. 2. Alignment and phylogenetic relationship between human TCTEX1D4 and its homologues. The protein sequences of TCTEX1D4 homologues were obtained from the Ensembl database by performing a Blastp search through the metazoans group using the human TCTEX1D4 sequence. (**A**) The chosen sequences were submitted to a ClustalW2 alignment. Open box indicate conservation of the RVSF motif across the placental mammals. (**B**) The resulting phylogenetic tree output was obtained by employing a Neighbor-Joining method with bootstrap test in MEGA program. *D. rerio* (zebrafish) was chosen as out-group. Scale bar: 0.05 substitutions per residue.

In order to test the direct interaction between TCTEX1D4 and PPP1, a membrane overlay was performed using bacterial cell lysates expressing recombinant TCTEX1D4 (Fig. 3C). The results show that TCTEX1D4 binds directly to both PPP1CC1 (upper panel) and PPP1CC2 (lower panel) purified proteins.

It is demonstrated that mutation of the PPP1BM either to AAxA (Liu et al., 2010), RAxA or to RVxA abolish the PPP1/PIP interaction, although some cases exist where interaction still occurs at a lesser extent (Bollen, 2001; Chang et al., 2002; Traweger et al., 2008; Wakula et al., 2006). We tested whether a
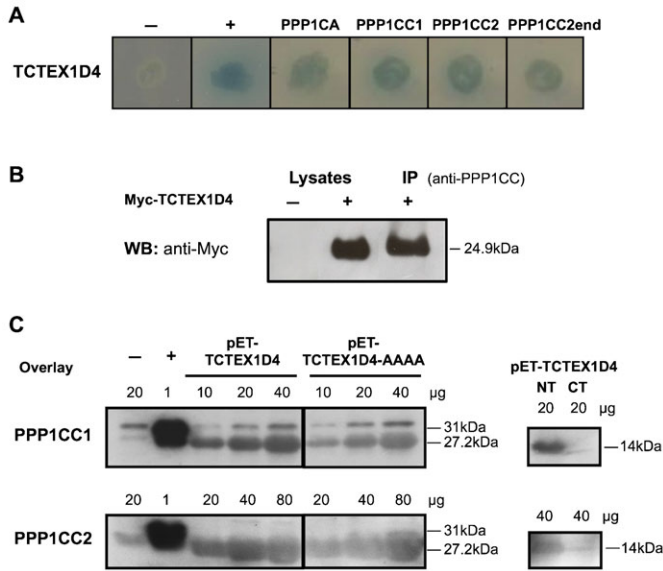
Fig. 3. **TCTEX1D4 binds to PPP1.** (A) Yeast co-transformation of pACT-2-TCTEX1D4 with PPP1CA, PPP1CC1, PPP1CC2 or PPP1CC2end in pAS2-1 vector, using the Li-Ac method. For negative and positive controls pAS2-1/pACT-2 and pVA3/pTD1 vectors were used, respectively. (**B**) Western blot showing that TCTEX1D4 binds to and co-immunoprecipitates PPP1CC in COS-7 cells transfected with Myc-TCTEX1D4. Non-transfected and transfected COS-7 cells were used as negative and positive controls, respectively. (**C**) Bacterial extracts expressing pET-TCTEX1D4, pET-TCTEX1D4-AAAA, pET-TCTEX1D4-NT (NT) and pET-TCTEX1D4-CT (CT) were run in an SDS-PAGE gel and overlaid with purified PPP1CC isoforms. pET vector alone was used as negative control and pET-NEK2C, a known PIP, was used as positive control. All experiments were repeated at least three times.

mutation of the TCTEX1D4 PPP1BM is crucial to the complex formation. The results reveal that mutation of the TCTEX1D4 PPP1BM RVSF to AAAA only partially reduces the binding (35%, pET-TCTEX1D4-AAAA lanes), with the same being true when RVSF is mutated to RVSA (data not shown). Furthermore, when using TCTEX1D4 N-terminus (NT) and C-terminus (CT) truncated forms in the overlay assay (Fig. 3C, right panel), it was shown that the important motifs for PPP1C binding, such as the RVSF, were present in the N-terminus portion of the TCTEX1D4 protein. However, it cannot be excluded that the C-terminus might be important for binding stabilization.

TCTEX1D4 expression in different tissues

By performing a NCBI EST database analysis with *TCTEX1D4* mRNA (NM_001013632.2) a total of 42 hits in *Sus scrofa*, *Rattus norvegicus*, *Mus musculus*, *Homo sapiens* and *Danio rerio* were retrieved. From the total ESTs identified, 45% corresponded to female reproductive tract related tissues (ovary, oviduct, placenta, uterus and embryonic tissue). Head related tissues (head, hypothalamus, brain, corpus striatum and tongue) corresponded to 21% and lung to 17% of the total ESTs. Moreover, in the databases no ESTs were found in testis, although it was already described in previous work by Northern blot (Meng et al., 2006).

A tissue screen of TCTEX1D4 protein expression was consequently performed on several rat tissues and human testis (Fig. 4). The results show that TCTEX1D4 is highly expressed in ovary, spleen, lung, placenta and kidney. It is also expressed in the other tissues tested, but in lower amounts, including human

testis. Interestingly, both antibodies, recognizing the N- or the C-terminus of TCTEX1D4, revealed the same immunoreactive profile, meaning that the two bands detected with each of the antibodies (24.9 and 28.4 kDa) correspond to the full-length TCTEX1D4.

Cellular localization of TCTEX1D4 in mouse testis and human spermatozoa

To validate the expression of TCTEX1D4 and to further specify the expression pattern in the testis we have performed immunohistochemical and qRT-PCR analyses on mouse testes. We found that TCTEX1D4 was expressed differentially (Fig. 5A). Within the seminiferous tubules, TCTEX1D4 immunoreactivity was localized in the basal part in a pattern that was typical for the blood–testis barrier (BTB) (Fig. 5D,G,J, arrows). The same pattern was shown after immunostaining of the testis with antibodies against Claudin-11 (Fig. 5C), which is an established marker for the BTB. In addition to the BTB localization, we found that TCTEX1D4 was expressed in spermatids in different patterns depending on the stage of seminiferous tubules. During the course of spermatid differentiation, TCTEX1D4 immunoreactivity was first observed in early elongating spermatids in a typical acrosome-like manner (Fig. 5J; stage X tubules, closed circles). This localization of TCTEX1D4 was consistent throughout spermiogenesis as shown in Fig. 5D,G. In late elongating spermatids, however, an additional strong focal immunoreactivity appeared in the cytoplasm of the spermatids. In late elongating spermatids of stage IV tubules, the immunoreactivity was within the adluminal cytoplasmic area (Fig. 5D, arrowheads) whereas the reactivity was shifted to the level of the nuclei of the almost mature spermatozoa at stage VII tubules (Fig. 5G, arrowheads). Specific immunostaining could not be observed in spermatocytes, peritubular myoid cells or in cells of the interstitial compartment of the testis. To test the specificity of TCTEX1D4 immunoreactivity, we also performed pre-absorption experiments. Prior to the regular immunostaining procedure, we incubated the polyclonal TCTEX1D4 antibody with a recombinant TCTEX1D4 peptide. The immunostaining was completely abolished indicating that the differential staining pattern that we observed was indeed reflecting the TCTEX1D4
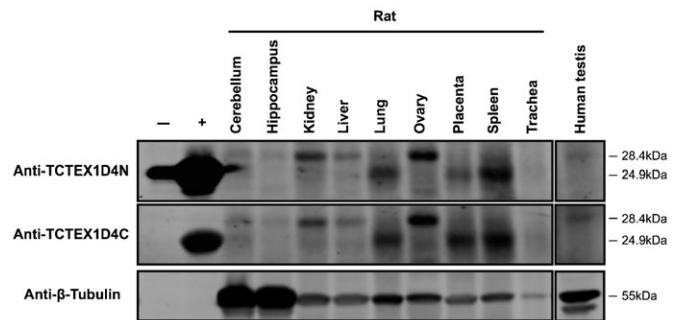

Fig. 4. **TCTEX1D4 protein expression profile.** Rat tissues and human testis extracts were prepared as described in Materials and Methods. A tissue protein expression profile (100 µg) of TCTEX1D4 was performed by Western blot using CBC8C (anti-TCTEX1D4C) and anti-TCTEX1D4N antibodies. The negative control consisted of bacterial extract expressing the pET vector alone, and the positive control of a bacterial extract expressing pET-TCTEX1D4. A loading control, β-tubulin, was also performed. Image shows representative blots from three independent experiments.
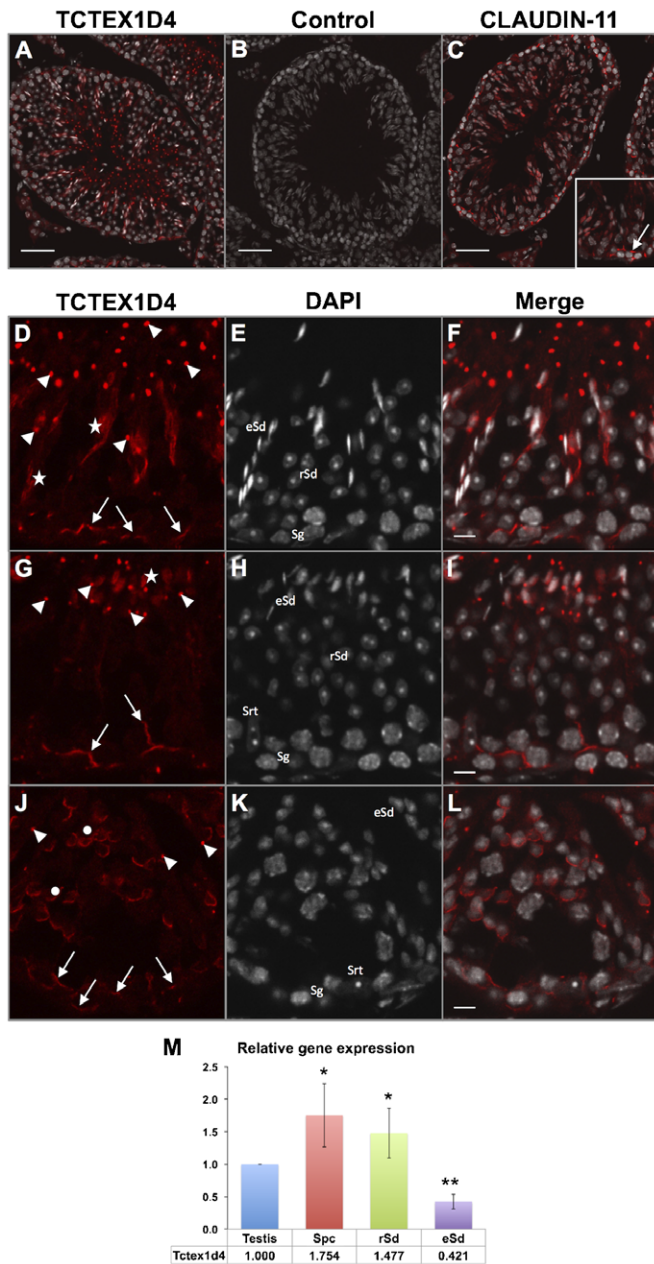
localization within the seminiferous tubules (Fig. 5B). Quantitative analysis of mRNA abundance in isolated germ cell populations by qRT-PCR revealed that relative expression levels of Tctex1d4 is elevated in spermatocytes fraction (Fig. 5M). This expression is maintained high in the round spermatids fraction being, however, markedly decreased in elongated spermatid fraction.

Given the presence of TCTEX1D4 in late stage germ cells, we further analyzed the subcellular localization of this protein in mature human sperm ejaculate (Fig. 6). The results show that TCTEX1D4 is present along the entire length of the flagellum, including principal and endpiece, and more predominantly in the midpiece region, where mitochondria are concentrated (Fig. 6A). TCTEX1D4 is also present in the head, particularly in the acrosome, but this pattern is only visible in some spermatozoa (Fig. 6A,B, asterisks). Of note, the subcellular localization pattern is similar when using either the N- or the C-terminus anti-TCTEX1D4 antibodies (data not shown). To confirm and further characterize TCTEX1D4 subcellular localization,
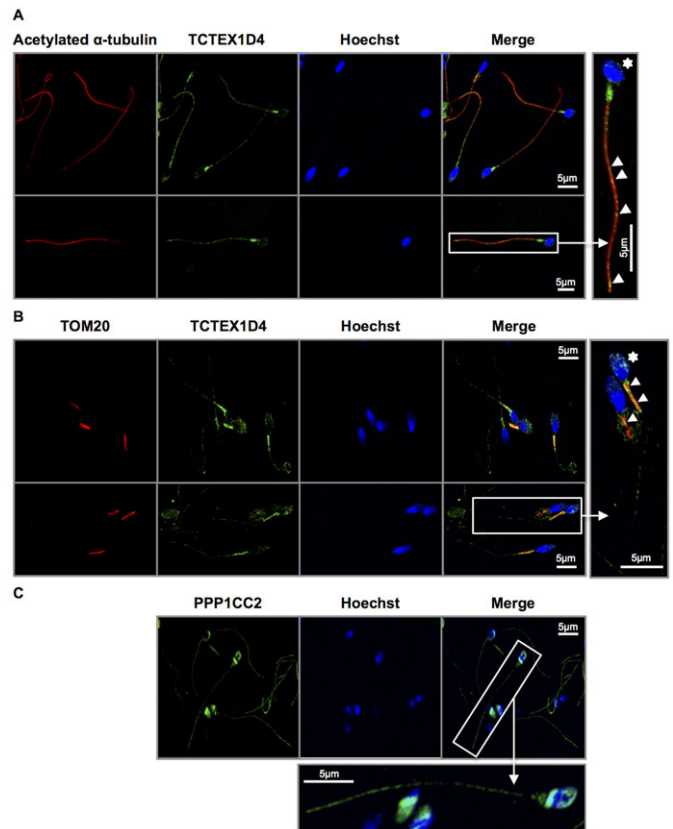

Fig. 5. TCTEX1D4 localization in testis. Mouse testis sections were stained with DAPI (nucleus, gray in A–C,E,F,H,I,K,L), and an anti-TCTEX1D4 antibody (CBC8C), and visualized by Cy3-labeled secondary antibody (red in A,B,D,F,G,I,J,L). (**A**) Mouse testis stained with antibodies to TCTEX1D4 (CBC8C) and Cy3-labeled secondary antibody. (**B**) TCTEX1D4 antibody pre-absorbed to a TCTEX1D4 peptide. (**C**) Mouse testis stained with antibodies to Claudin-11 and Cy3-labeled secondary antibody for visualization of the BTB. Different stages of spermatid differentiation are shown as enlarged images: (**D–F**) stage IV, (**G–I**) stage VII and (**J–L**) stage X. Overlays of DAPI and Cy3 staining are shown in A–C,F,I,L. Arrows indicate the BTB, asterisks indicate late elongating spermatids, closed circles indicate acrosome-like structures of early elongating spermatids and arrowheads point to focal regions within the spermatid cytoplasm. (**M**) Relative expression values for the isolated cell fractions were calculated by the ΔΔ Ct-method. *Increased mRNA expression compared to the control (testis) above 1.5-fold or below 0.75-fold. **Changes in expression levels of more than 2-fold or below 0.5-fold. Sg, spermatogonia; Spc, spermatocyte; rSd, round spermatid; eSd, elongated spermatid; Srt, Sertoli cell. Scale bars: 50 µm in A–C and 10 µm in F,I,L.

Fig. 6. TCTEX1D4 subcellular localization in human sperm. (**A**) Human ejaculate sperm was stained with α-tubulin (anti-acetylated-α-tubulin, red), TCTEX1D4 (CBC8C, green) and nucleus (Hoechst, blue), and subjected to confocal microscopy analysis. ROI image on the right is shown for an easier visualization of the co-localization in the axoneme (white arrowheads) and in the acrosome (white asterisks). (**B**) Spermatozoa were stained for mitochondria (TOM20, red), TCTEX1D4 (CBC8C, green) and nucleus (Hoechst, blue). ROI image on the right is shown for an easier visualization of the co-localization in the midpiece (white arrowheads) and in the acrosome (white asterisks). (**C**) Spermatozoa were stained for PPP1CC2 (CBC502, green) and nucleus (Hoechst, blue). ROI image on the bottom is shown for a closer visualization of the PPP1CC2 localization. Images are representative of three independent experiments. All images were obtained at 100× magnification. Scale bars: 5 µm.

antibodies against the axonemal component tubulin (anti-acetylated-α-tubulin) and mitochondria (TOM20) were used (Fig. 6A,B, respectively). Merged images clearly show that TCTEX1D4 co-localizes with axoneme and mitochondria. Relatively to the potential subcellular sites of PPP1CC2-TCTEX1D4 co-localization in human sperm, PPP1CC2 was observed in the posterior, equatorial and acrosomal regions of the head and along the entire flagellum, including the mid-piece, upon sperm staining with the CBC502 antibody (Fig. 6C). This is the expected PPP1CC2 sperm distribution and past work from our laboratory has shown the interaction of PPP1CC2 with β-tubulin by mass spectrometry in human sperm (Fardilha et al., 2011b).

TCTEX1D4 and PPP1 co-localize at MTOC/microtubules in mammalian cells

A Myc-TCTEX1D4 construct and mouse anti-Myc antibodies were used to confirm TCTEX1D4 subcellular localization and address TCTEX1D4-PPP1 co-localization in mammalian cells. The subcellular localization of transfected TCTEX1D4 was first analyzed in a spermatogonia cell line, GC1-spg, where TCTEX1D4 was detected in the nucleus and cytoplasm, being enriched in the MTOC and in the emergent microtubules. These data are confirmed by the co-localization with specific subcellular markers: centrin, that specifically stains the centrioles present in MTOC, and β-tubulin, that stains the microtubules (Fig. 7A).

To further characterize the TCTEX1D4-PPP1 holoenzyme, COS-7 cells were transfected with Myc-TCTEX1D4 and stained with anti-Myc (TCTEX1D4 detection, red) and CBC3C (endogenous PPP1 detection, green) antibodies (Fig. 7B). Again, TCTEX1D4 was observed in the cell nucleus and cytoplasm, where it was present in microtubules and enriched in the MTOC (Fig. 7B). PPP1CC co-localizes with TCTEX1D4 mainly in these regions: inside the nucleus and in the MTOC (Fig. 7B). Interestingly, PPP1CC also accompanies TCTEX1D4 in the microtubules emerging from the MTOC, suggesting that TCTEX1D4-PPP1CC binding might be important for PPP1CC microtubular localization. In order to address this hypothesis, we used the Myc-TCTEX1D4-RVSA mutant that is characterized by a 35% decrease in the TCTEX1D4-PPP1CC binding (Fig. 3C). Remarkably, PPP1CC/TCTEX1D4-RVSA co-localized to a much lower extent in the MTOC and along the microtubules emerging from the MTOC (Fig. 7B). This is clearly indicated by the fluorescence intensity profiles (Fig. 7C) representing the voxels through the white arrows indicated in Fig. 7B microphotographs. The PPP1CC signal was particularly decreased in both the MTOC and in microtubules, suggesting that TCTEX1D4 is at least partially responsible for PPP1C MTOC/microtubular localization/transport. Results were further confirmed by quantitative correlation analysis of PPP1CC/TCTEX1D4 co-localization percentages in the cytoplasm of TCTEX1D4 transfected cells (Fig. 7D). While the percentage of cytoplasmic PPP1CC co-localized with TCTEX1D4 decreased by ~34% (from 41.5 ± 2.5 to $27.5\pm2.7\%$), when the RVSF motif was mutated to RVSA the percentage of the TCTEX1D4 cytoplasmic pool co-localizing with PPP1CC also decreased by ~27% (85.9 ± 1.3 to $62.7\pm2.2\%$). Furthermore, the percentage of transfected cells in which PPP1CC/TCTEX1D4 co-localizes decreased 3-fold in case of the TCTEX1D4-RVSA mutant. Essentially, both PPP1CC localization at the MTOC and its

microtubular transport appear to be dependent on PPP1CC binding to the dynein LC TCTEX1D4.

Discussion

The present work gives an insight into the putative role of the dynein light chain protein TCTEX1D4 within the testis. TCTEX1D4 forms a complex with PPP1CC2, a phosphatase that was shown to play a role in sperm motility (Fardilha et al., 2011a). The PPP1-TCTEX1D4 interaction was first identified by a yeast two-hybrid approach. The results were further confirmed by overlay and co-immunoprecipitation techniques (Fig. 3). TCTEX1D4 has a PPP1 binding motif that is evolutionarily conserved among species (Fig. 2). Studies with TCTEX1D4 PPP1-binding mutants strengthened the importance of this PPP1 interaction motif for complex formation (Fig. 3C). The only dynein light chain that processes a putative motif, besides TCTEX1D4, is TCTEX1D3 ([150]KVLF[153]), but the motif is mapped to the globular domain Tctex1, which might be masked and thus not as easily accessible for PPP1 binding as for TCTEX1D4 (Fig. 1B,C). Functionally, while the ICs/LCs form the cargo complex, the LC confer specificity to this binding (Lo et al., 2007; Tai et al., 1999), regulate other molecules or stabilize the assembly of the motor dynein complex (DiBella et al., 2005). PPP1CC is known to bind to and dephosphorylate the IC (Whyte et al., 2008), and most probably PPP1 binding to TCTEX1D4 would facilitate its access and binding to the IC. Furthermore, PPP1 may additionally dephosphorylate TCTEX1D4 itself, and therefore regulate its function. Of note, TCTEX1D4 has a comparatively longer disordered N-terminus (Fig. 1B,C) that potentially gives it a more flexible and exposed arm to bind different cargo and diverse regulatory proteins, as well as being regulated by reversible phosphorylation.

Serine phosphorylation appears to be the most relevant post-translational modification for TCTEX1D4, with several putative target kinases identified, supporting the relevance of its binding to the Ser/Thr phosphatase PPP1 (Fig. 1A). Also, the results of the putative binding sites for cyclins and MAPK reinforce the Ser24 phosphorylation site predicted for cyclin/CDK complex and MAPK, which sustain a possible role for TCTEX1D4 in the cell cycle, proliferation and differentiation processes, also controlled by the TGFβ signaling pathway (Tian and Schiemann, 2009). However, the binding sites for cyclins and MAPK are localized in the globular domain; thus, the motifs' availability, for example in loops within the globular domain, requires further confirmation (Fig. 1A). In contrast to TCTEX1, TCTEX1D2 and TCTEX1D3 that have orthologs in *Chlamydomonas* genus (DiBella et al., 2004; Harrison et al., 1998; Pazour et al., 1999), TCTEX1D4 emerged only in vertebrates, possibly by duplication, which may suggest the gain of novel and specialized functions for this protein in this phylum (Fig. 2). One of these functions might imply the binding to PPP1. Interestingly, the TCTEX1D4 PPP1BM emerged in the placental mammals at the same time as PPP1CC2, the testis enriched and sperm specific isoform. The TCTEX1D4 binding mutants experiment show a decrease in binding but not a complete loss. This may be explained by the unusual sequence surrounding the TCTEX1D4 RVSF motif, which is similar to a palindrome with a high percentage of prolines – **P**SLG**P**V**P***PLGS*<u>RVSF</u>*SGLP***L**A**P**A**R**W**V**A**P** (**bold**: prolines; *italic*: palindrome; <u>underlined</u>: PPP1BM). This sequence is likely to form a structured arm forcing towards the RVSF
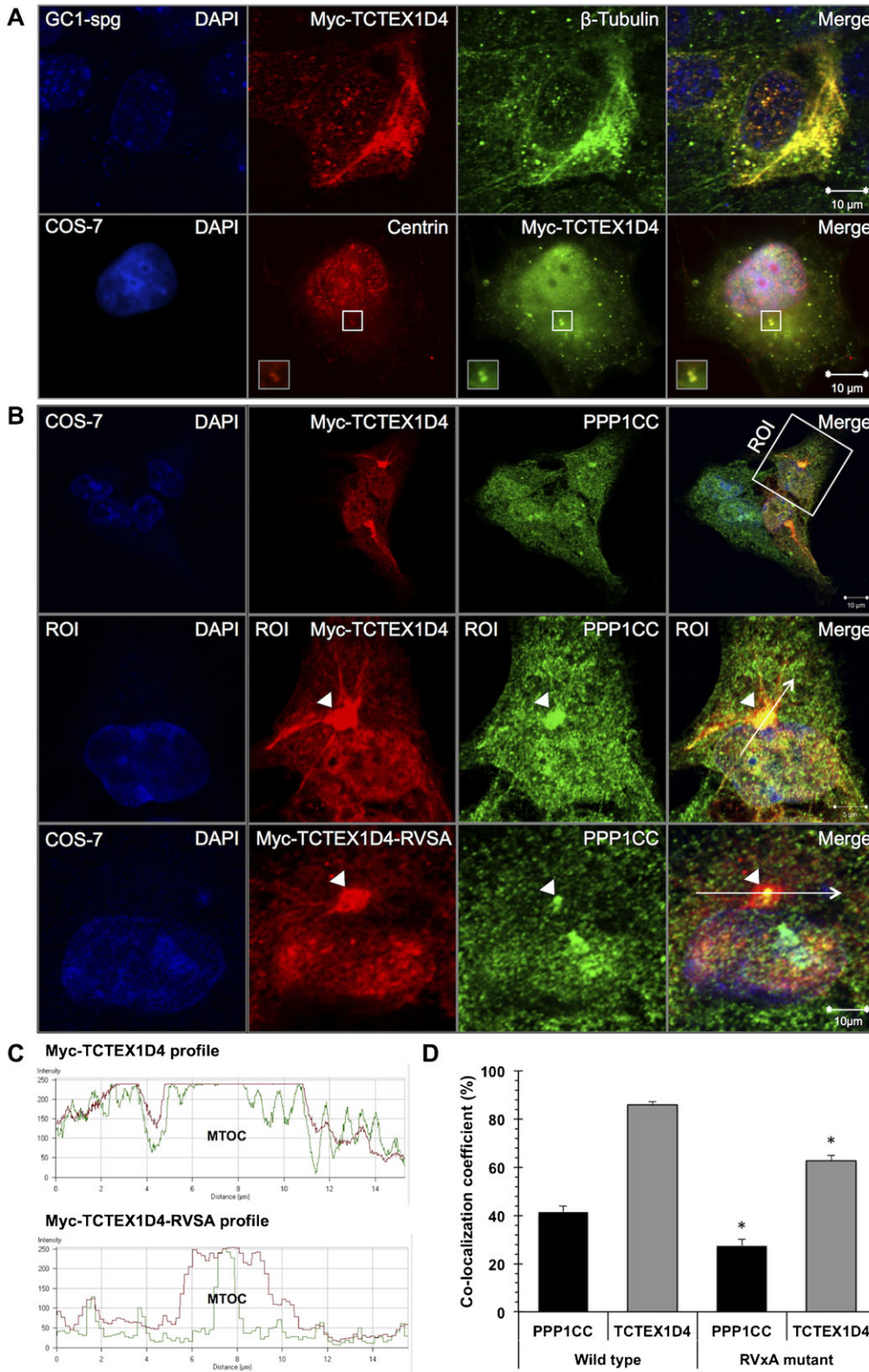
Fig. 7. **TCTEX1D4-PPP1 binding regulates the localization of the holoenzyme at microtubules and MTOC.** (**A**) GC1-spg cells (top) and COS-7 cells (bottom) were transfected with Myc-TCTEX1D4, labeled with anti-Myc and Texas-Red anti-mouse antibodies. GC1-spg cells were also immunostained with anti-β-tubulin antibody to visualize microtubules (confocal microscopy analysis), while COS-7 cells were immunostained with anti-centrin antibody to label the microtubule organizing center (MTOC) (epifluorescence microscopy analysis). All images are at 100× magnification. Scale bars: 10 µm. Negative controls only with secondary antibodies were performed (data not shown). (**B**) COS-7 cells were transfected with wild-type Myc-TCTEX1D4 or the Myc-TCTEX1D4-RVSA mutant, which has reduced ability to bind PPP1C. Arrowhead indicates MTOC. All images are at 100× magnification and were visualized in a confocal microscope. Scale bars: 10 µm (top and bottom rows), 5 µm (middle row). White arrows indicate the profiles localization. (**C**) Fluorescence intensity profiles representing the voxels through the white arrowed lines indicated in B. (**D**) Co-localization coefficients were determined for the percentage of PPP1CC co-localizing with TCTEX1D4 (black columns), and the percentage of TCTEX1D4 co-localizing with PPP1CC (gray columns), in cells transfected either with wild-type (Myc-TCTEX1D4) or mutated (Myc-TCTEX1D4-RVSA) TCTEX1D4. Results were plotted and significant differences were found (*$P<0.001$; $n=15$).

motif, even when it is mutated to AAAA, to enter the PPP1 hydrophobic pocket to which the RVxF motif is known to bind. It is possible that RVSF ablation leads to the destruction of the arm, and consequently to the ablation of TCTEX1D4-PPP1 binding, but this needs further proof. Another possible hypothesis to explain the observed partial reduction in binding is that other important binding sites, which are not yet described, could also be present.

TCTEX1D4 tissue expression profile indicated that the protein is expressed in several tissues, but to a higher extent in ovary,

spleen, lung and placenta, where PPP1 is also present (da Cruz e Silva et al., 1995) (Fig. 4). These results are in agreement with the EST *TCTEX1D4* profile, and also with previous results, describing *TCTEX1D4* in a human placenta cDNA library by yeast two-hybrid and by RT-PCR in human testis and placenta (Meng et al., 2006). Since the predicted molecular mass of TCTEX1D4 is 23.4 kDa, the observed band shift from 24.9 kDa to 28.4 kDa most probably results from post-translational modifications in the predicted sites, such as phosphorylations and/or glycosylations (Fig. 1A).

By immunofluorescence analysis we showed that TCTEX1D4 is expressed differentially in the seminiferous tubules of mouse testis. TCTEX1D4 is enriched at the cell–cell junctions of the BTB. It is stated that TCTEX1D4 interacts with endoglin and TGFβRII receptors in placenta and in Hela cells (Meng et al., 2006). Also, in Mv1Lu cells TCTEX1D4 inhibits both TGFβ1/3 signaling by increasing the retention time of both receptors at the cell surface and blocking their internalization (Meng et al., 2006). TGFβ signaling has also been shown to participate in the regulation of the BTB physiology (Xia et al., 2005; Xia et al., 2009). Although the BTB is one of the tightest blood–tissue barriers, it has some permeability in the stages VIII to IX of the germ cell cycle to allow for the migration of preleptotene/ leptotene spermatocytes into the adluminal compartment. The current hypothesis is that the internalization (endocytosis) and recycling events are evenly balanced. However, during the stages VIII to IX the internalization event is increased leading to an imbalance and a permissive BTB (Xia et al., 2009). Cytokines, TGFβ3 and TNFα, were already shown to be involved in these phenomenon by increasing endocytosis of the membrane receptors (Li et al., 2006; Xia et al., 2006; Xia et al., 2009; Xia and Cheng, 2005). Therefore, TCTEX1D4 might have an important role in the regulation of the BTB, either by preventing higher levels of receptor internalization and thereby maintaining the balance before the stages VIII to IX, or by stopping the effect of the cytokines and re-establishing the balance after the preleptotene/leptotene spermatocytes migration. TCTEX1D4 is also present in spermatids in an acrosome-like pattern and in focal regions of the cytoplasm (Fig. 5). The acrosome-like pattern might indicate a role in the acrosome cap formation whereas the focal cytoplasmic staining might indicate the preassembly of the axonemal components within the cytoplasm or cytoplasmic droplets with excess cytoplasm targeted for removal. These localization patterns resemble that of focal adhesion kinase (FAK) protein that displays phosphorylation-dependent localization in the testes (Lie et al., 2012). The immunohistochemistry and qRT-PCR analysis suggest that *Tctex1d4* mRNA level is increased in spermatocytes, being only translated in round spermatids since no significant staining was seen in these germ cells (Fig. 5). This delay between transcription and translation events is common in testis (Hecht, 1998; Idler and Yan, 2012). Also, during spermatid differentiation a strong downregulation of this gene was observed (Fig. 5M). Furthermore, immunocytochemistry analysis confirmed that TCTEX1D4 is present in mature spermatozoa, particularly in the flagellum, being enriched in the midpiece region (Fig. 6A,B). The differential expression and the multiple subcellular localizations of TCTEX1D4 in testicular cells may indicate that TCTEX1D4 has several functions. Based on our data, TCTEX1D4 has yet unknown functions at the BTB but is involved in the spermatid differentiation in mouse testis. The

co-localization with microtubules in Cos7 cells and in human spermatozoa suggests a role of TCTEX1D4 in both organelle rearrangements and protein transport (cytoplasmic functions) and in ciliar/flagellar motility (axonemal functions). Similar functions have been described for its family member DYNLT1, which is both axonemal and cytoplasmic (Harrison et al., 1998; King et al., 1996). In sperm immunofluorescence microphotographs it is difficult to distinguish between different structures, thus it remains unclear whether TCTEX1D4 will have a role in the axoneme apparatus flagellar function (for sperm motility) or as a minus-end cytoplasmic dynein motor in the intraflagellar transport (IFT) (Patel-King et al., 1997) (Fig. 6A). IFT is a motility event in flagella, unrelated to dynein-based motility, which has been observed as a bidirectional transportation of granule-like particles along the length of flagella (Kozminski et al., 1993). According to both PPP1C and TCTEX1D4 distribution in sperm, the localization of the TCTEX1D4/PPP1CC2 complex appears to be primarily restricted to the flagellum and to a lesser extent in the head (Fig. 6). This suggests a putative role for the TCTEX1D4-PPP1CC2 holoenzyme in sperm motility, where TCTEX1D4 could have its dynein functions altered by PPP1CC2 dephosphorylation and/or would function to transport PPP1CC2 to other possible motility-related PPP1C targets. Studies in rainbow trout and chum salmon sperm have shown that a TCTEX1D3 homologue (LC2) of the outer dynein arm is phosphorylated when sperm is activated (Inaba et al., 1999) and that dephosphorylation by PPP2 induces immotility in sperm (Inaba, 2002). This model could be similar to what happens in human sperm with TCTEX1D4 and PPP1CC2 (Fig. 8). Since mammalian sperm contains a different isoform of PPP1C, the sperm-specific PPP1CC2, and TCTEX1D4 only appeared in vertebrates, this dynein light chain could be the effector of PPP1CC2 activity in mammals, inducing sperm immotility. Fig. 8 depicts other possible functions of the complex TCTEX1D4/PPP1CC2 in sperm physiology.

Furthermore, PPP1 and TCTEX1D4 co-localize in the MTOC and microtubules, and TCTEX1D4 appears to be at least partially responsible for PPP1 transport along microtubules and PPP1 targeting to MTOC (Fig. 7). This localization is consistent with the role of TCTEX1D4 as a dynein LC thus linked to microtubules and responsible for PPP1C microtubule-dependent retrograde transport. In this way, TCTEX1D4 may regulate PPP1 functions since PPP1 localization at microtubules is important to regulate microtubule dynamics (e.g. in mitosis (Tournebize et al., 1997)) and to regulate cargo transport, by mediating cargo dissociation from the kinesin motor unit (Morfini et al., 2004; Morfini et al., 2002). Of note, only part of the TCTEX1D4 cytoplasmic pool is associated with microtubules, as it was also reported to occur for TCTEX1, suggesting several distinct roles for these proteins (Tai et al., 1998). The presence of TCTEX1D4 in the microtubules and MTOC is in accordance with the previous immunohistochemistry observations, and strongly suggests a role for TCTEX1D4 in microtubules organization and dynamics. Indeed, dyneins were previously shown to have an important role in MTOC cellular positioning, re-orientation throughout the cell cycle and migration, and in microtubule dynamics (Gönczy et al., 1999; Palazzo et al., 2001; Schmoranzer et al., 2009).

Interestingly, the testis protein TLRR (lrrc67), found in the MTOC of germ cells and in cell cultures (Wang et al., 2010), binds to PPP1CC2, β-tubulin, KIF5B (Kinesin-1B), DYNC1I1,
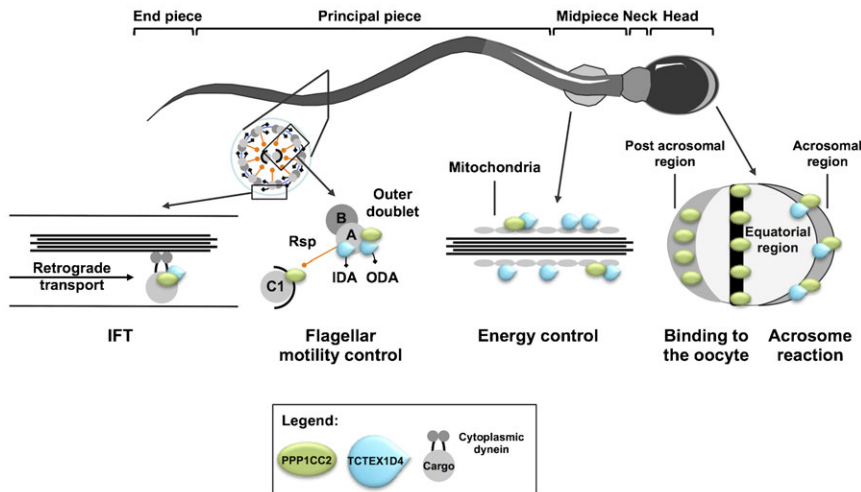
Fig. 8. Schematic representation of TCTEX1D4 and TCTEX1D4-PPP1CC2 localization in sperm. TCTEX1D4 is present in the head and along the tail of human mature spermatozoa. PPP1CC2 is present in the posterior, equatorial and acrosome regions of the head, as well as in the entire tail, including midpiece. PPP1 was shown to be present in the central pair apparatus axoneme, associated with the C1 microtubule, and to a lesser extent in the outer doublet microtubules, in *Chlamydomonas*. The diagram shows the putative roles that could be assigned to TCTEX1D4 (and the TCTEX1D4-PPP1CC2 complex) at these locations. In the head, TCTEX1D4 may have a role in the acrosome reaction, while along the tail it could have a function in sperm flagellar motility and/or in vesicular intraflagellar transport (IFT). In the midpiece, where mitochondria are concentrated and TCTEX1D4 is highly enriched, TCTEX1D4 may be involved in the energy production necessary for the flagellar motility. Rsp, radial spoke; C1, central pair microtubule 1; B, tubule B; A, tubule A; IDA, inner dynein arm; ODA, outer dynein arm.

and was suggested to have a role in sperm flagellum formation (Wang et al., 2010). The authors further proposed that the TLRR-PPP1CC2 complex regulates the activity of the (plus end) kinesin-1B motor unit in testis. In light of our studies, we suggest that the TCTEX1D4-PPP1CC2 complex may function in the opposite direction, regulating the (minus end) motor unit dynein that comprises TCTEX1D4 as its LC. Additional questions regarding the specific role of this complex in spermatogenesis and sperm physiology will require further work, but will provide new insight into the biology of human reproduction.

Materials and Methods
Plasmid constructs
Construction of plasmids was carried out as described previously (Wu et al., 2007). The following plasmids were prepared:

pAS2-PPP1CA – *PPP1CA* cDNA was directionally subcloned into *Eco*RI/*Bam*HI digested pAS2-1 (Clontech, Saint Germain-en-Laye, France) to produce pAS2-PPP1CA.

pAS2-PPP1CC1 – *PPP1CC1* cDNA was directionally subcloned into *Sal*I/*Sma*I digested pAS2-1 (Clontech, Saint Germain-en-Laye, France) to produce pAS2-PPP1CC1.

pAS2-PPP1CC2/pAS2-PPP1CC2end – The 200 bp *PPP1CC2*-specific C-terminus-containing *Pst*I fragment was transferred from pTacTac-PPP1CC2 into *Pst*I digested pAS-PPP1CC2 to produce pAS-PPP1CC2 or into *Pst*I digested pAS2-1 to produce pAS-PPP1CC2end (Fardilha et al., 2004). The pAS2-PPP1CC constructs were used in the yeast two-hybrid screening.

pET-TCTEX1D4 – *TCTEX1D4* cDNA was PCR-amplified forward (5′-gcgaattcatggccagcaggcctc-3′) and reverse (5′-ccgctcggtcactcgcagtagagc-3′) from clone IMAGE 30531412 and inserted into pET-28a vector (Novagen, Madison, Wisconsin, USA).

pET-TCTEX1D4-NT/CT – The N-terminus portion of the *TCTEX1D4* cDNA was PCR amplified with pET forward primer and an internal reverse primer (5′-ccgctcgagtcaggcgggcgccaggg-3′). The pET-TCTEX1D4-NT construct comprises amino acids 1–101. Likewise, the C-terminus portion of the *TCTEX1D4* cDNA was PCR amplified with an internal forward primer (5′-gcgaattccgttgggtggcgcc-3′) and pET reverse primer. The pET-TCTEX1D4-CT construct comprises amino acids 102–221. The pET-TCTEX1D4 and NT and CT constructs were used in the overlay assay for PPP1C binding.

Myc-TCTEX1D4 – *TCTEX1D4* cDNA was PCR-amplified from pET-TCTEX1D4 with primers forward (5′-gcgaattccgatggccagcaggcctc-3′) and reverse (5′-ccgctcggtcactcgcagtagagc-3′), and inserted into *Eco*RI/*Xho*I sites of pCMV-Myc vector (Clontech, Saint Germain-en-Laye, France). This construct was used in immunoprecipitation and immunofluorescence.

pACT-TCTEX1D4 – *TCTEX1D4* cDNA was digested from Myc-TCTEX1D4 with *Eco*RI/*Xho*I, and inserted into *Eco*RI/*Xho*I digested pACT-2 (Clontech, Saint Germain-en-Laye, France), using standard molecular biology procedures. The pACT-TCTEX1D4 and pAS2-PPP1C constructs were used in the co-transformation assay. The pAS2-1/pACT-2 and the pVA3/pTD1 vectors (Clontech, Saint Germain-en-Laye, France) were used as co-transformation controls.

pET-TCTEX1D4-AAAA/Myc-TCTEX1D4-RVSA – Mutagenesis of PPP1BM RVSF in *TCTEX1D4* cDNA was performed using the QuikChange Site-Directed Mutagenesis Kit (Stratagene, now Agilent Technologies UK Ltd, Edinburgh, UK) by mutating just the last or all the four amino acids to alanine in order to disrupt the PPP1BM. The pET-TCTEX1D4-AAAA was used in the overlay assay, whereas Myc-TCTEX1D4-RVSA construct was used in immunofluorescence studies.

Antibodies
The mouse anti-Myc tag (Cell Signaling, Danvers, Massachusetts, USA), the mouse acetylated anti-α-tubulin (Zymed Laboratories Inc., Cambridge, UK), the mouse anti-β-tubulin (Zymed Laboratories Inc., Cambridge, UK) and the rabbit anti-TCTEX1D4N (N-terminus of TCTEX1D4, PGGQRPSLGPVPPLGSR-VSFSGLPLAPARWVAPSYRTEPVPGERWEAARA, Sigma–Aldrich Química, S.A., Sintra, Portugal) antibodies were purchased from the respective companies. The antibodies CBC3C (against the C-terminus of PPP1CC, detects both isoforms (da Cruz e Silva et al., 1995)), CBC502 (specific for the C-terminus of PPP1CC2) and CBC8C (C-terminus of TCTEX1D4, WDVARDGLA-SVSYTNTSLFAVATVHGLYCE) were raised in rabbit and were already described (Browne et al., 2007; Fardilha et al., 2008; Ouimet et al., 1995; Vijayaraghavan et al., 1996). The mouse TOM20 (translocase of outer membrane 20 kDa subunit) antibody was a kind gift of Dr Michael Schrader (University of Aveiro, Aveiro, Portugal) (Delille and Schrader, 2008).

Yeast two-hybrid screening
The methods for yeast two-hybrid screening of a human testis cDNA library using human PPP1C have been described previously (Browne et al., 2007; Fardilha et al., 2011b; Fardilha et al., 2004).

Bioinformatics analysis
Full protein sequences of intermediate chains (ICs), light intermediate chains (LICs) and light chains (LCs) were obtained from Ensembl database to check for PPP1 binding motifs. The ICs human homologues are: the axonemal inner arm IC1 (ENSP00000242317) and IC2 (ENSP00000308312), axonemal outer arm IC138 (ENSP00000360065) and IC140 (ENSP00000294664), and cytoplasmic DYNC1I1 (ENSP00000320130), DYNC1I2 (ENSP00380308). The LICs human homologues are the cytoplasmic DYNC1LI1 (ENSP00000273130), DYNC1LI2 (ENSP00000258198) and cytoplasmic from intraflagellar transport DYNC2LI1 (ENSP00000330752). The LCs human homologues are the DYNLRB1/LC7/Roadblock (NP_054902.1), DYNLRB2/LC7/Roadblock (ENSP00000302936), DYNLL1/LC8 (ENSP00000376297), DYNLL2/LC8 (ENSP00000240343), TXNDC3/LC5 (ENSP00000199447), TXNDC6/LC5 (ENSP00000372667), DNAL1/LC1 (ENSP00000310360), DNAL4/LC6 (ENSP00000216068) DYNLT1/Tctex1, DYNLT3/RP3, TCTEX1D1, TCTEX1D2/Tctex2b, TCTEX1D3/Tctex2/Tcte3, and TCTEX1D4/Tctex2β. The last 6 comprise the Tctex1 family and the respective Ensembl IDs are depicted in the alignment Fig. 2A. Eukaryotic Linear Motif (ELM) (Puntervoll et al., 2003), Psipred (Jones, 1999), ScanProsite (ExPASy Proteomics Server), NetPhos, and NetNGlyc1.0 (CBS Prediction Servers) search engines were used to further characterize relevant motifs and post-translational modifications. For homology and evolutionary purposes, ClustalW2 and MEGA programs were used (Larkin et al., 2007; Tamura et al., 2011).

Yeast co-transformation

Yeast competent AH109 cells were co-transformed with pACT-TCTEX1D4 and pAS2-PPP1CA, pAS2-PPP1CC1, pAS2-PPP1CC2 or pAS2-PPP1CC2end, by the lithium acetate method (Fardilha et al., 2011b; Fardilha et al., 2004). Afterwards, the transformation mixture was plated on selective media containing X-α-Gal and incubated at 30℃ to check for MEL1 expression as indicated by the appearance of a blue color (Clontech, Saint Germain-en-Laye, France).

Co-immunoprecipitation and TCTEX1D4 tissue expression screening

African green monkey (*Cercopithecus aethiops*) SV40-transformed kidney cells (COS-7, fibroblast-like, ATCC CRL-1651, Manassas, Virginia, USA) were grown in the appropriate medium (DMEM) and transfected with Myc-TCTEX1D4, harvested and lysed in lysis buffer (50 mM Tris-HCl, 120 mM NaCl, 4% CHAPS, 0.1 mg/ml Pepstatin A, 0.03 mM Leupeptin, 145 mM Benzamidine, 0.37 mg/ml Aprotinin and 4.4 mM PMSF in isopropanol). The lysates were pre-cleared with protein A sepharose slurry (Pharmacia, LKB Biotechnology, Bromma, Sweden) for 1 hour at 4℃ with shaking. After centrifugation, protein sepharose and CBC3C (2 µg) were added to the supernatant, followed by overnight incubation at 4℃ with shaking. Subsequently, the beads were washed three times with 50 mM Tris-HCl, 120 mM NaCl and resuspended in loading buffer. Samples were loaded in SDS-PAGE gel, and transferred to a nitrocellulose membrane. Immunodetection was performed using anti-Myc antibody (1:5000). For the tissue screening, tissues from adult Wistar rat strain (2–3 months) and human testis were lysed using a homogenizer in 1% SDS. Human testis biopsies were collected *in vivo*, in Hospital Central (Centro Hospitalar de Coimbra, Coimbra, Portugal), during procedures to collect organs for transplantation from adult healthy man donors. Biopsies for research purposes are covered by the legislation of the Portuguese Constitution (decreto-lei no. 274/99 of 22 July 1999). Both CBC8C (1:100) and anti-TCTEX1D4N (1:1000) antibodies were used in separate blots for immunodetection of protein expression. Immunoreactive bands were detected by enhanced chemiluminescence (ECL, GE Healthcare, Amersham Biosciences Europe GmbH, Freiburg, Germany) (Fardilha et al., 2007).

Overlay assays

A single *Rosetta* (DE3) (Novagen, Madison, Wisconsin, USA) colony expressing His-tagged TCTEX1D4 was selected and grown overnight in 3 ml Luria Bertani medium containing ampicillin (50 µg/ml) at 37℃. Expression was induced with 0.1 mM isopropyl-β-D-thio-galactopyranoside at 37℃. Samples were then treated as described elsewhere (Browne et al., 2007). The same procedure was also performed for TCTEX1D4-AAAA, TCTEX1D4-NT and TCTEX1D4-CT. Blots were overlaid with purified PPP1CC1 or PPP1CC2 (25 pmol/ml) and detected with CBC3C (1:5000) (Browne et al., 2007).

Immunohistochemistry

For fluorescence microscopy analysis, cryosections were prepared. C57/Bl6 mice testes were fixed by perfusion with 4% paraformaldehyde, 0.1 M HEPES, pH 7.4 and immersed in 0.1 M phosphate buffer at room temperature for 6 hours, followed by immersion in 30% (w/v) sucrose solution at 4℃ overnight. The tissue was frozen in isopentane at −30℃ and stored at −80℃. Cryosections of about 8–10 µm were cut using a Cryostat (Leica Biosystems, Wetzlar, Germany). For immunohistochemistry, tissue sections were initially rehydrated and permeabilized in TBS-TT (TBS with 0.2% Triton-X and 0.2% Tween 20) for 30 minutes and then incubated with 10% (v/v) Roti-Block (Roth, Karlsruhe, Germany; diluted in dH₂O) for 1 hour to reduce non-specific binding of antibodies. Sections were further incubated with primary antibodies against TCTEX1D4 (CBC8C, 1:150) or Claudin-11 (Claudin-11/OSP anti-rabbit; polyclonal antibody, Invitrogen, diluted 1:150) in 10% (v/v) Roti-Block in PBS for 1 hour at room temperature. After extensive washing with TBS, tissue sections were incubated with a secondary antibody (Cy3-conjugated goat anti rabbit IgG, diluted 1:500, Sigma, Taufkirchen, Germany) suspended in 10% (v/v) Roti-Block, for 1 hour, to visualize immune complexes. For DNA labeling, the secondary antibody was supplemented with 1 µg/ml 4′,6-Diamidino-2-phenylindole (DAPI, Gibco BRL). Sections were washed in TBS and mounted with Mowiol 4–88 (Roth). Specimens were analyzed using Nikon Instruments A1 Confocal Laser Microscope with standard filters for detection of Cy3 and DAPI. Digital images were obtained with a Nikon A1plus camera using the Nikon NIS Elements Advanced Research software. The use of mice was in accordance with the Guide for the Care and Use of Laboratory Animals from the Institute for Laboratory Animal Research. The local Ethics Committee approved the study and the procedures were in compliance with the current national laws.

Expression analysis in isolated testicular germ cells

Isolation of cell populations from mouse testis was performed as described elsewhere (Dastig et al., 2011). Isolated cells were analyzed by phase contrast microscopy and DAPI staining, and homogeneous cell populations were used for further analysis. Isolated cells were processed for RNA isolation (RNeasy mini kit, Qiagen, Hilden, Germany). Total RNA from the isolated cells was prepared using the RNeasy Plus Universal Midi Kit (Quiagen, Germany). The concentration of RNA was determined spectrophotometrically (NanoDrop 1000 Spectrophotometer, Thermo Scientific, Germany). For synthesis of cDNA, a reverse transcription reaction was carried out using 1 µg of RNA and the Transcriptor First Strand cDNA Synthesis Kit (Roche, Germany). Expression levels of distinct mRNAs were determined by qRT-PCR using the LightCycler 480 SYBR Green I Master (Roche, Germany) on 96-well plates with the LightCycler® 480 Real-Time PCR System (Roche, Germany) as already described (Dastig et al., 2011). A combination of *Gapdh* and *Hprt* was used as reference genes for the testis and all expression levels were calculated as relative values using the mean of both reference genes. The samples were run in triplicate and the averages were used for calculation of expression levels of the different genes. The expression quantification of the *Tctex1d4* gene was calculated as described before (Dastig et al., 2011) using the forward (5′-aggcacacagccccaatctgac-3′) and the reverse (5′-agccaggtctttggtagtctcctc-3′) primers. A cDNA obtained from the cell suspension of whole testis was used as control sample for qRT-PCR reactions. Markers specific for each germ cell were used to further reconfirm the purity of the isolated germ cells. All primers are listed in supplementary material Table S1.

Immunocytochemistry

GC1-spg (ATCC CRL-2053, Manassas, Virginia, USA) and COS-7 cell lines were grown using previously established conditions (da Cruz e Silva et al., 2004). GC1-spg are *Mus musculus* (strain BALB/c) type B spermatogonia cells, epithelial-like, that show characteristics of a stage between type B spermatogonia and primary spermatocytes. Cells were transfected with Myc-TCTEX1D4 or Myc-TCTEX1D4-RVSA with Lipofectamine 2000 (Invitrogen, Life Technologies S.A., Madrid, Spain) using standard procedures (Vieira et al., 2010; Wu et al., 2007). Preparation of cells for immunochemistry was achieved by cold methanol fixation as described previously (Fardilha et al., 2007). Human ejaculated sperm was first washed three times in PBS, diluted and applied to coated coverslips. Subsequent steps were similar to those applied for the COS-7 cells. Ejaculated sperm was collected from healthy donors by masturbation into an appropriate sterile container (informed consents were signed allowing samples to be used for scientific purposes). Spermograms were performed by experienced technicians and only samples with normal parameters were used (World Health Organization, 1999). For all methods, sperm was washed three times in 1× PBS. Anti-Myc (1:5000), CBC3C (1:1000), CBC8C (1:100) and CBC502 (1:1000) primary antibodies were used to detect the respective proteins. Fluorescent secondary antibodies anti-mouse Texas-Red (1:300) and anti-rabbit Alexa488 (1:300) were subsequently used. Nuclei were stained with Hoechst 33258 (1:2000, Polysciences Europe GmbH, Eppelheim, Germany) or DAPI (1:200, Vectashield, Vector Laboratories Burlingame, California, USA). Fluorescence images were acquired in an Olympus IX-81 inverted epifluorescence microscope (Olympus Portugal – Opto-Digital Tecnologias, S.A., Lisboa, Portugal) using a ×100 objective, or on a Zeiss LSM-510 confocal microscope (Carl Zeiss Ltd, Wetzlar, Germany). For confocal microscopy, quantitative correlation analysis of PPP1CC and wild-type and mutant TCTEX1D4 was carried out with the Zeiss LSM 510 4.0 software (Vieira et al., 2010), using images of delimited TCTEX1D4 transfected single cells. The co-localization coefficients were determined as the percentage of PPP1CC/TCTEX1D4 co-localizing pixels relatively to the number of pixels in the PPP1CC and in the TCTEX1D4 channels.

Statistical analysis

SigmaPlot statistical package (SigmaPlot v.11, Systat Software Inc.) was used for statistical analysis. The Kolmogorov–Smirnov test was employed to test normality of distribution of the data. Significant differences between co-localization coefficients were evaluated with the unpaired Student's t-test ($P < 0.001$, alpha=0.050).

Competing Interests

The authors have no competing interests to declare.

References

Allen, P. B., Greenfield, A. T., Svenningsson, P., Haspeslagh, D. C. and Greengard, P. (2004). Phactrs 1–4: A family of protein phosphatase 1 and actin regulatory proteins. *Proc. Natl. Acad. Sci. USA* **101**, 7187-7192.

Bollen, M. (2001). Combinatorial control of protein phosphatase-1. *Trends Biochem. Sci.* **26**, 426-431.

Browne, G. J., Fardilha, M., Oxenham, S. K., Wu, W., Helps, N. R., da Cruz E Silva, O. A. B., Cohen, P. T. and da Cruz E Silva, E. F. (2007). SARP, a new alternatively spliced protein phosphatase 1 and DNA interacting protein. *Biochem. J.* **402**, 187-196.

Chang, J. S., Henry, K., Wolf, B. L., Geli, M. and Lemmon, S. K. (2002). Protein phosphatase-1 binding to scd5p is important for regulation of actin organization and endocytosis in yeast. *J. Biol. Chem.* **277**, 48002-48008.

Cohen, P. T. (2002). Protein phosphatase 1 – targeted in many directions. *J. Cell Sci.* **115**, 241-256.

da Cruz e Silva, E. F., Fox, C. A., Ouimet, C. C., Gustafson, E., Watson, S. J. and Greengard, P. (1995). Differential expression of protein phosphatase 1 isoforms in mammalian brain. *J. Neurosci.* **15**, 3375-3389.

da Cruz e Silva, O. A. B., Vieira, S. I., Rebelo, S. and da Cruz e Silva, E. F. (2004). A model system to study intracellular trafficking and processing of the Alzheimer's amyloid precursor protein. *Neurodegener. Dis.* **1**, 196-204.

Dastig, S., Nenicu, A., Otte, D. M., Zimmer, A., Seitz, J., Baumgart-Vogt, E. and Lüers, G. H. (2011). Germ cells of male mice express genes for peroxisomal metabolic pathways implicated in the regulation of spermatogenesis and the protection against oxidative stress. *Histochem. Cell Biol.* **136**, 413-425.

Delille, H. K. and Schrader, M. (2008). Targeting of hFis1 to peroxisomes is mediated by Pex19p. *J. Biol. Chem.* **283**, 31107-31115.

DiBella, L. M., Smith, E. F., Patel-King, R. S., Wakabayashi, K. and King, S. M. (2004). A novel Tctex2-related light chain is required for stability of inner dynein arm I1 and motor function in the *Chlamydomonas* flagellum. *J. Biol. Chem.* **279**, 21666-21676.

DiBella, L. M., Gorbatyuk, O., Sakato, M., Wakabayashi, K., Patel-King, R. S., Pazour, G. J., Witman, G. B. and King, S. M. (2005). Differential light chain assembly influences outer arm dynein motor function. *Mol. Biol. Cell* **16**, 5661-5674.

Fardilha, M., Wu, W., Sá, R., Fidalgo, S., Sousa, C., Mota, C., da Cruz e Silva, O. A. B. and da Cruz e Silva, E. F. (2004). Alternatively spliced protein variants as potential therapeutic targets for male infertility and contraception. *Ann. N. Y. Acad. Sci.* **1030**, 468-478.

Fardilha, M., Vieira, S. I., Barros, A., Sousa, M., Da Cruz e Silva, O. A. B. and Da Cruz e Silva, E. F. (2007). Differential distribution of Alzheimer's amyloid precursor protein family variants in human sperm. *Ann. N. Y. Acad. Sci.* **1096**, 196-206.

Fardilha, M., da Cruz e Silva, O. A. B. and da Cruz e Silva, E. F. (2008). A importância do mecanismo de "splicing" alternativo para a identificação de novos alvos terapêuticos. [Article in Portuguese]. *Acta Urológica* **25**, 39-47.

Fardilha, M., Esteves, S. L. C., Korrodi-Gregório, L., da Cruz e Silva, O. A. B. and da Cruz e Silva, F. F. (2010). The physiological relevance of protein phosphatase 1 and its interacting proteins to health and disease. *Curr. Med. Chem.* **17**, 3996-4017.

Fardilha, M., Esteves, S. L. C., Korrodi-Gregório, L., Pelech, S., da Cruz E Silva, O. A. B. and da Cruz E Silva, E. (2011a). Protein phosphatase 1 complexes modulate sperm motility and present novel targets for male infertility. *Mol. Hum. Reprod.* **17**, 466-477.

Fardilha, M., Esteves, S. L. C., Korrodi-Gregório, L., Vintém, A. P., Domingues, S. C., Rebelo, S., Morrice, N., Cohen, P. T. W., da Cruz e Silva, O. A. B. and da Cruz e Silva, E. F. (2011b). Identification of the human testis protein phosphatase 1 interactome. *Biochem. Pharmacol.* **82**, 1403-1415.

Gönczy, P., Pichler, S., Kirkham, M. and Hyman, A. A. (1999). Cytoplasmic dynein is required for distinct aspects of Mtoc positioning, including centrosome separation, in the one cell stage *Caenorhabditis elegans* embryo. *J. Cell Biol.* **147**, 135-150.

Harrison, A., Olds-Clarke, P. and King, S. M. (1998). Identification of the *t* complex-encoded cytoplasmic dynein light chain tctex1 in inner arm I1 supports the involvement of flagellar dyneins in meiotic drive. *J. Cell Biol.* **140**, 1137-1147.

Hecht, N. B. (1998). Molecular mechanisms of male germ cell differentiation. *Bioessays* **20**, 555-561.

Hendrickx, A., Beullens, M., Ceulemans, H., Den Abt, T., Van Eynde, A., Nicolaescu, E., Lesage, B. and Bollen, M. (2009). Docking motif-guided mapping of the interactome of protein phosphatase-1. *Chem. Biol.* **16**, 365-371.

Idler, R. K. and Yan, W. (2012). Control of messenger RNA fate by RNA-binding proteins: an emphasis on mammalian spermatogenesis. *J. Androl.* **33**, 309-337.

Inaba, K. (2002). Dephosphorylation of Tctex2-related dynein light chain by type 2A protein phosphatase. *Biochem. Biophys. Res. Commun.* **297**, 800-805.

Inaba, K., Kagami, O. and Ogawa, K. (1999). Tctex2-related outer arm dynein light chain is phosphorylated at activation of sperm motility. *Biochem. Biophys. Res. Commun.* **256**, 177-183.

Jones, D. T. (1999). Protein secondary structure prediction based on position-specific scoring matrices. *J. Mol. Biol.* **292**, 195-202.

Kao, S. C., Chen, C. Y., Wang, S. L., Yang, J. J., Hung, W. C., Chen, Y. C., Lai, N. S., Liu, H. T., Huang, H. L., Chen, H. C. et al. (2007). Identification of phostensin, a PP1 F-actin cytoskeleton targeting subunit. *Biochem. Biophys. Res. Commun.* **356**, 594-598.

King, S. M., Dillman, J. F., 3rd, Benashski, S. E., Lye, R. J., Patel-King, R. S. and Pfister, K. K. (1996). The mouse *t*-complex-encoded protein Tctex-1 is a light chain of brain cytoplasmic dynein. *J. Biol. Chem.* **271**, 32281-32287.

Kozminski, K. G., Johnson, K. A., Forscher, P. and Rosenbaum, J. L. (1993). A motility in the eukaryotic flagellum unrelated to flagellar beating. *Proc. Natl. Acad. Sci. USA* **90**, 5519-5523.

Lai, N. S., Wang, T. F., Wang, S. L., Chen, C. Y., Yen, J. Y., Huang, H. L., Li, C., Huang, K. Y., Liu, S. Q., Lin, T. H. et al. (2009). Phostensin caps to the pointed end of actin filaments and modulates actin dynamics. *Biochem. Biophys. Res. Commun.* **387**, 676-681.

Larkin, M. A., Blackshields, G., Brown, N. P., Chenna, R., McGettigan, P. A., McWilliam, H., Valentin, F., Wallace, I. M., Wilm, A., Lopez, R. et al. (2007). Clustal W and Clustal X version 2.0. *Bioinformatics* **23**, 2947-2948.

Li, M. W. M., Xia, W., Mruk, D. D., Wang, C. Q. F., Yan, H. H. N., Siu, M. K. Y., Lui, W. Y., Lee, W. M. and Cheng, C. Y. (2006). Tumor necrosis factor α reversibly disrupts the blood–testis barrier and impairs Sertoli–germ cell adhesion in the seminiferous epithelium of adult rat testes. *J. Endocrinol.* **190**, 313-329.

Lie, P. P., Mruk, D. D., Mok, K. W., Su, L., Lee, W. M. and Cheng, C. Y. (2012). Focal adhesion kinase-Tyr[407] and -Tyr[397] exhibit antagonistic effects on blood–testis barrier dynamics in the rat. *Proc. Natl. Acad. Sci. USA* **109**, 12562-12567.

Liu, D., Vleugel, M., Backer, C. B., Hori, T., Fukagawa, T., Cheeseman, I. M. and Lampson, M. A. (2010). Regulated targeting of protein phosphatase 1 to the outer kinetochore by KNL1 opposes Aurora B kinase. *J. Cell Biol.* **188**, 809-820.

Lo, K. W., Kogoy, J. M. and Pfister, K. K. (2007). The DYNLT3 light chain directly links cytoplasmic dynein to a spindle checkpoint protein, Bub3. *J. Biol. Chem.* **282**, 11205-11212.

Meng, Q., Lux, A., Holloschi, A., Li, J., Hughes, J. M., Foerg, T., McCarthy, J. E., Heagerty, A. M., Kioschis, P., Hafner, M. et al. (2006). Identification of Tctex2β, a novel dynein light chain family member that interacts with different transforming growth factor-β receptors. *J. Biol. Chem.* **281**, 37069-37080.

Morfini, G., Szebenyi, G., Elluru, R., Ratner, N. and Brady, S. T. (2002). Glycogen synthase kinase 3 phosphorylates kinesin light chains and negatively regulates kinesin-based motility. *EMBO J.* **21**, 281-293.

Morfini, G., Szebenyi, G., Brown, H., Pant, H. C., Pigino, G., DeBoer, S., Beffert, U. and Brady, S. T. (2004). A novel CDK5-dependent pathway for regulating GSK3 activity and kinesin-driven motility in neurons. *EMBO J.* **23**, 2235-2245.

Ouimet, C. C., da Cruz e Silva, E. F. and Greengard, P. (1995). The alpha and gamma 1 isoforms of protein phosphatase 1 are highly and specifically concentrated in dendritic spines. *Proc. Natl. Acad. Sci. USA* **92**, 3396-3400.

Palazzo, A. F., Joseph, H. L., Chen, Y. J., Dujardin, D. L., Alberts, A. S., Pfister, K. K., Vallee, R. B. and Gundersen, G. G. (2001). Cdc42, dynein, and dynactin regulate MTOC reorientation independent of Rho-regulated microtubule stabilization. *Curr. Biol.* **11**, 1536-1541.

Patel-King, R. S., Benashski, S. E., Harrison, A. and King, S. M. (1997). A *Chlamydomonas* homologue of the putative murine *t* complex distorter Tctex-2 is an outer arm dynein light chain. *J. Cell Biol.* **137**, 1081-1090.

Pazour, G. J., Koutoulis, A., Benashski, S. E., Dickert, B. L., Sheng, H., Patel-King, R. S., King, S. M. and Witman, G. B. (1999). LC2, the *Chlamydomonas* homologue of the *t* complex-encoded protein Tctex2, is essential for outer dynein arm assembly. *Mol. Biol. Cell* **10**, 3507-3520.

Pazour, G. J., Agrin, N., Walker, B. L. and Witman, G. B. (2006). Identification of predicted human outer dynein arm genes: candidates for primary ciliary dyskinesia genes. *J. Med. Genet.* **43**, 62-73.

Puntervoll, P., Linding, R., Gemünd, C., Chabanis-Davidson, S., Mattingsdal, M., Cameron, S., Martin, D. M., Ausiello, G., Brannetti, B., Costantini, A. et al. (2003). ELM server: a new resource for investigating short functional sites in modular eukaryotic proteins. *Nucleic Acids Res.* **31**, 3625-3630.

Schmoranzer, J., Fawcett, J. P., Segura, M., Tan, S., Vallee, R. B., Pawson, T. and Gundersen, G. G. (2009). Par3 and dynein associate to regulate local microtubule dynamics and centrosome orientation during migration. *Curr. Biol.* **19**, 1065-1074.

Tai, A. W., Chuang, J. Z. and Sung, C. H. (1998). Localization of Tctex-1, a cytoplasmic dynein light chain, to the Golgi apparatus and evidence for dynein complex heterogeneity. *J. Biol. Chem.* **273**, 19639-19649.

Tai, A. W., Chuang, J. Z., Bode, C., Wolfrum, U. and Sung, C. H. (1999). Rhodopsin's carboxy-terminal cytoplasmic tail acts as a membrane receptor for cytoplasmic dynein by binding to the dynein light chain Tctex-1. *Cell* **97**, 877-887.

Tamura, K., Peterson, D., Peterson, N., Stecher, G., Nei, M. and Kumar, S. (2011). MEGA5: molecular evolutionary genetics analysis using maximum likelihood, evolutionary distance, and maximum parsimony methods. *Mol. Biol. Evol.* **28**, 2731-2739.

Tian, M. and Schiemann, W. P. (2009). The TGF-β paradox in human cancer: an update. *Future Oncol.* **5**, 259-271.

Tournebize, R., Andersen, S. S. L., Verde, F., Dorée, M., Karsenti, E. and Hyman, A. A. (1997). Distinct roles of PP1 and PP2A-like phosphatases in control of microtubule dynamics during mitosis. *EMBO J.* **16**, 5537-5549.

Traweger, A., Wiggin, G., Taylor, L., Tate, S. A., Metalnikov, P. and Pawson, T. (2008). Protein phosphatase 1 regulates the phosphorylation state of the polarity scaffold Par-3. *Proc. Natl. Acad. Sci. USA* **105**, 10402-10407.

Vaughan, P. S., Leszyk, J. D. and Vaughan, K. T. (2001). Cytoplasmic dynein intermediate chain phosphorylation regulates binding to dynactin. *J. Biol. Chem.* **276**, 26171-26179.

Vieira, S. I., Rebelo, S., Esselmann, H., Wiltfang, J., Lah, J., Lane, R., Small, S. A., Gandy, S., da Cruz E Silva, E. F. and da Cruz E Silva, O. A. B. (2010). Retrieval of the Alzheimer's amyloid precursor protein from the endosome to the TGN is S655 phosphorylation state-dependent and retromer-mediated. *Mol. Neurodegener.* **5**, 40.

Vijayaraghavan, S., Stephens, D. T., Trautman, K., Smith, G. D., Khatra, B., da Cruz e Silva, E. F. and Greengard, P. (1996). Sperm motility development in the

epididymis is associated with decreased glycogen synthase kinase-3 and protein phosphatase 1 activity. *Biol. Reprod.* **54**, 709-718.

Virshup, D. M. and Shenolikar, S. (2009). From promiscuity to precision: protein phosphatases get a makeover. *Mol. Cell* **33**, 537-545.

Wakula, P., Beullens, M., van Eynde, A., Ceulemans, H., Stalmans, W. and Bollen, M. (2006). The translation initiation factor eIF2β is an interactor of protein phosphatase-1. *Biochem. J.* **400**, 377-383.

Wang, R., Kaul, A. and Sperry, A. O. (2010). TLRR (lrrc67) interacts with PP1 and is associated with a cytoskeletal complex in the testis. *Biol. Cell* **102**, 173-189.

Whyte, J., Bader, J. R., Tauhata, S. B., Raycroft, M., Hornick, J., Pfister, K. K., Lane, W. S., Chan, G. K., Hinchcliffe, E. H., Vaughan, P. S. et al. (2008). Phosphorylation regulates targeting of cytoplasmic dynein to kinetochores during mitosis. *J. Cell Biol.* **183**, 819-834.

Wirschell, M., Hendrickson, T. and Sale, W. S. (2007). Keeping an eye on I1: I1 dynein as a model for flagellar dynein assembly and regulation. *Cell Motil. Cytoskeleton* **64**, 569-579.

World Health Organization. (1999). Collection and examination of human semen. In *WHO Laboratory For Examination Of Human Semen And Sperm–Cervical Mucus Interaction*, 4th edition, pp. 4-30. Cambridge: Cambridge University Press.

Wu, W., Baxter, J. E., Wattam, S. L., Hayward, D. G., Fardilha, M., Knebel, A., Ford, E. M., da Cruz e Silva, E. F. and Fry, A. M. (2007). Alternative splicing controls nuclear translocation of the cell cycle-regulated Nek2 kinase. *J. Biol. Chem.* **282**, 26431-26440.

Xia, W. and Cheng, C. Y. (2005). TGF-β3 regulates anchoring junction dynamics in the seminiferous epithelium of the rat testis via the Ras/ERK signaling pathway: an *in vivo* study. *Dev. Biol.* **280**, 321-343.

Xia, W., Mruk, D. D., Lee, W. M. and Cheng, C. Y. (2005). Cytokines and junction restructuring during spermatogenesis—a lesson to learn from the testis. *Cytokine Growth Factor Rev.* **16**, 469-493.

Xia, W., Mruk, D. D., Lee, W. M. and Cheng, C. Y. (2006). Differential interactions between transforming growth factor-β3/TβR1, TAB1, and CD2AP disrupt blood-testis barrier and Sertoli-germ cell adhesion. *J. Biol. Chem.* **281**, 16799-16813.

Xia, W., Wong, E. W. P., Mruk, D. D. and Cheng, C. Y. (2009). TGF-β3 and TNFα perturb blood–testis barrier (BTB) dynamics by accelerating the clathrin-mediated endocytosis of integral membrane proteins: a new concept of BTB regulation during spermatogenesis. *Dev. Biol.* **327**, 48-61.

Yang, P., Fox, L., Colbran, R. J. and Sale, W. S. (2000). Protein phosphatases PP1 and PP2A are located in distinct positions in the *Chlamydomonas* flagellar axoneme. *J. Cell Sci.* **113**, 91-102.